# Large-Strain Softening of Aluminum in Shear at Elevated Temperature

M.E. KASSNER, M.Z. WANG, M.-T. PEREZ-PRADO, and S. ALHAJERI

Pure aluminum deformed in pure shear at elevated temperature reaches a broad "peak" stress and then undergoes about a 17 pct decrease in flow stress with deformation with, roughly, 1 to 2 equivalent uniaxial strain. Beyond this strain, the flow stress is approximately constant. The sources for this softening are unclear. The suggested basis includes texture softening, microstructural softening, enhanced dynamic recovery, and discontinuous dynamic recrystallization. Experiments were performed in which specimens were deformed in torsion to various strains within the softening regime followed by compression tests at ambient and elevated temperature. Analysis of the compressive yield strengths indicate that the softening is most likely substantially explained by a decrease in the average Taylor factor.

## I. INTRODUCTION

THE stress *vs* strain behavior and microstructural evolution of aluminum deformed in pure shear (*e.g.*, torsion) at elevated temperatures has been studied by a variety of groups including Myshlyaev and co-workers,[1–4] Monthiellet and co-workers,[5,6,7], McQueen *et al.*,[8–12] Pettersen *et al.*,[13,14] and Kassner *et al.*[15–19]

The ductility of high and commercial purity Al can exceed, in torsion, equivalent uniaxial strains of 100. Typically, the Al hardens to a peak stress $\overline{\sigma}_{p,ss}$ at strains less than 0.5. The flow stress subsequently decreases to a flow stress, $\overline{\sigma}_{ss}$, which is nearly constant and a steady-state condition is reached. The peak stress, $\overline{\sigma}_{p,ss}$, seems essentially equivalent to the steady-state creep stress observed in tension. It is generally agreed that under pure shear, such as with torsion tests, the flow stress decreases by about 17 pct and this occurs over a fairly broad range of 1 to 2 strain, depending on the temperature and strain rate, as illustrated in Figure 1.[18] This softening has not been widely attributed to discontinuous dynamic recrystallization (DRX), which often evinces softening in the flow behavior, rather only dynamic recovery (DRV) is widely accepted to occur, although Yamagata[20] insists that DRX occurs with high-temperature deformation of high-purity aluminum in compression, but this has not been reproduced by any other group. (The softening of 17 pct to strains of 1 to 2 is often followed by a slight, gradual, increase in torque (about 4 pct) above strains of about 10.[18]) The cause of the softening is not fully understood. Explanations vary from decreases in the average Taylor factor (textural softening) to changes in the dislocation substructure (*e.g.*, increase in the average subgrain size), sometimes through increased dynamic recovery, to DRX. It is now widely agreed that large strain deformation results in a dramatic increase in the high-angle boundary (HAB) area. That is, one-third to one-half of the initially low-misorientation subgrain facets become HABs ($\theta > 8$ deg). Two groups[8–12,15–19] attribute this primarily to geometric dynamic recrystallization (GDX), where the original grains of the polycrystalline-aggregate elongate, increase HAB area, and "replace" the subgrain boundaries with HABs. These HABs have ancestry to the HABs of the starting polycrystal. Others have considered the formation to be additionally, or primarily, due to continuous reactions (continuous dynamic recrystallization) where subgrains gradually transform to HABs resulting from dislocation accumulation.[5,6,7,13] The formation of HABs in single crystals was confirmed to occur in Al at high temperatures and not as a consequence of DRX.[15,19] Thus, HABs can form in some cases from dislocation reaction. The number of HABs in the single crystal, however, was much less than for large strain deformation of polycrystals (9 pct *vs* 35 pct). The boundaries in the single crystal may be geometric necessary boundaries (GNBs), which are HABs that form from dislocation reaction and occur as incompatible slip occurs in a given grain/crystal.[6,21,22] Thus, GDX may be more important in terms of forming HABs, at least in pure polycrystalline Al and probably other alloys as well.[8,23] Figure 2 illustrates the microstructural evolution with large strain deformation of high-purity aluminum at 371 °C and a strain rate of $5.04 \times 10^{-4}$ s$^{-1}$, based on earlier work by one of the authors.[16,18] The figure illustrates that both the subgrain size and the dislocation density (not associated with subgrain boundaries) are approximately constant throughout deformation. The figure shows that the equiaxed subgrains have an increased fraction (up to about one-third) of facets that become HABs. This fraction was constant over the range tested, 4 to 16. (The original $\overline{\sigma}$-$\overline{\varepsilon}$ curve[16] was modified once more accurate data were obtained.[18])

Pettersen and Nes[14] recently suggested that the softening in aluminum alloys (AA 6060 and 6082) is a result of these new HABs being particularly effective sinks or annihilation sites for dislocations, leading to softening from larger subgrain sizes. More specifically, the softening is due to a combination of factors, including a decrease in strength due to a decrease in the average Taylor factor, as well as to changes

M.E. KASSNER, Northwest Aluminum Professor, and M.Z. WANG, Research Associate, are with the Department of Mechanical Engineering, Oregon State University, Corvallis, OR 97331. Contact email: kassner@engr.orst.edu M.-T. PEREZ-PRADO, Research Associate, Department of Mechanical Engineering, Oregon State University, is Researcher, CENIM, CSIC, Madrid, Spain. S. ALHAJERI, formerly Research Assistant, Department of Mechanical Engineering, Oregon State University, is Assistant Professor, Production Department, Kuwait Institute of Technology, Kuwait City, Kuwait.

Manuscript submitted October 25, 2001.

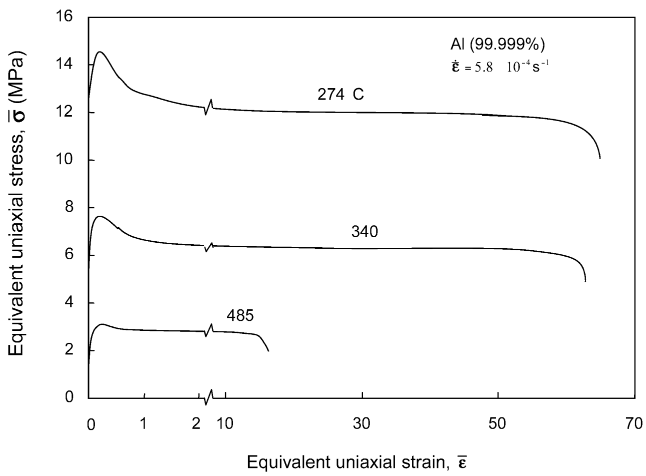


(*a*)

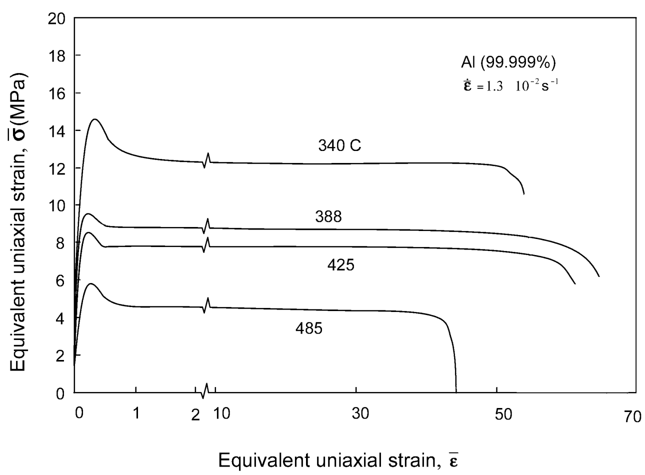


(*b*)

Fig. 1—The elevated-temperature equivalent-uniaxial stress *vs* equivalent-uniaxial strain of high-purity Al at strain rates of (*a*) $5.8 \times 10^{-4}$ s$^{1}$ and (*b*) $1.3 \times 10^{-2}$.[18]

in the size of the subgrains with increased subgrain size accounting for most (approximately two-thirds) of the softening. Perdrix *et al.*[5] suggested that softening can originate from three sources: the decrease in Taylor factor, increase in subgrain size, and a small increase in stress exponent. It does not appear that these investigators quantify the relative contributions to softening, but do suggest that the Taylor factor decreases by about 18 pct, enough to rationalize all of the softening. These investigators, as did Pettersen *et al.*[13,14] (but not Kassner and McMahon[16]), noticed an increase in subgrain size with strain. McQueen[12] appears to rationalize the softening exclusively by texture. One problem with this microstructural-based explanation is that it appears that changes in the subgrain size in Al, by itself, do not seem to affect the flow stress, as discussed extensively in Reference 24. Pettersen also suggested that a significant fraction of the HABs formed from dislocation reactions, such as with GNBs. Kassner and co-workers[16,25] found that for pure Al and Al5.8 pct Mg, the fraction of HABs as a function of strain is consistent with GDX and that GNB or boundaries forming from continuous reactions do not comprise a dominating fraction of HABs after very large strains.

The softening has not been attributed to any new deformation mechanism that might arise from the increase in HAB area, such as Coble creep or an increased contribution to strain from grain boundary sliding (GBS). This is largely due to the observations that the activation energy for creep plasticity is unchanged from that of self-diffusion, and the stress exponent is unchanged from that of about 4 to 5 over the softening regime.[4,5] Either Coble or GBS would be associated with smaller stress exponents (1 to 2) and activation energies about half that of lattice self-diffusion.

Pettersen found that the textures and corresponding Taylor factors (M) for some hot-deformed aluminum alloys were, based on X-ray and orientation imaging microscopy (OIM) analysis, $A^2$, C, and $B^1$, where $A^2$ was observed to be relatively weak, and M is unreported, as shown in Table I. Pettersen based the preceding Taylor factors on slip that included non-traditional systems (the M values were converted, for ease of comparison, to equivalent tension values, or $M_T$). The first index is the crystallographic plane in the shear plane and the second is the shear direction. McQueen *et al.*[9,10] observed the A, $B^1$, and C textures in commercial purity Al deformed in torsion to large strains at 400 °C, with the $B^1$ being strongest. Later, McQueen[12] only observed the strong $B^1$ texture based on X-ray diffraction and scanning transmission electron microscopy on pure Al. Perdrix *et al.*[5] noted the softest (111) [$1\bar{1}0$] or A texture at a strain of 31 in commercial purity Al at 400 °C. Barnett and Montheillet,[6] most recently, examined the textures by electron backscattered diffraction from strains of 0 to 2 (softening regime), and concluded that four texture components were developing, A, $A^2$, B, and C in Al 1050 at 450 °C, of equal magnitude, with about 30 pct of material within 10 deg of the texture components. Kocks *et al.*[26] discuss textures in pure metals torsionally deformed at ambient and elevated temperatures. They emphasize that B and (weak) A fiber torsion textures are common. Shrivastava *et al.*[27] calculated the torsional Taylor factors using the Bishop and Hill (traditional slip systems) method for A, C, and $B^1$ textures. These are also listed in Table I. The average value was 2.39, or about 16 pct less than 2.86 for a random array of aggregates. If the strongest ($B^1$) texture and the"traditional" Taylor factors are used, a decrease in Taylor factor from 2.86 to 2.44 is expected, leading to a flow stress decrease of 15 pct. Pettersen argued that the "harder" C component texture that she observed in addition to the $B^1$ texture in the aluminum alloy only mandated a decrease in flow stress of 5 to 7 pct, with, again, the remaining softening resulting from increased dynamic recovery in association with the dramatic increase in HABs. Thus, the common conclusion is that torsion deformation of aluminum is associated with decreases in the average Taylor factor.

The purpose of the work in the present investigation is to assess the contribution of DRX, HABs, and especially texture (average Taylor factor) on the softening behavior of aluminum deformed in torsion to relatively large strains at elevated temperatures. This will be, especially, accomplished by performing compression tests subsequent to torsion tests to various strains within the softening regime. If (isotropic) microstructural effects rationalize the torsion softening, then the compressive yield stress will decrease with torsional prestrain (compression axis coincident with

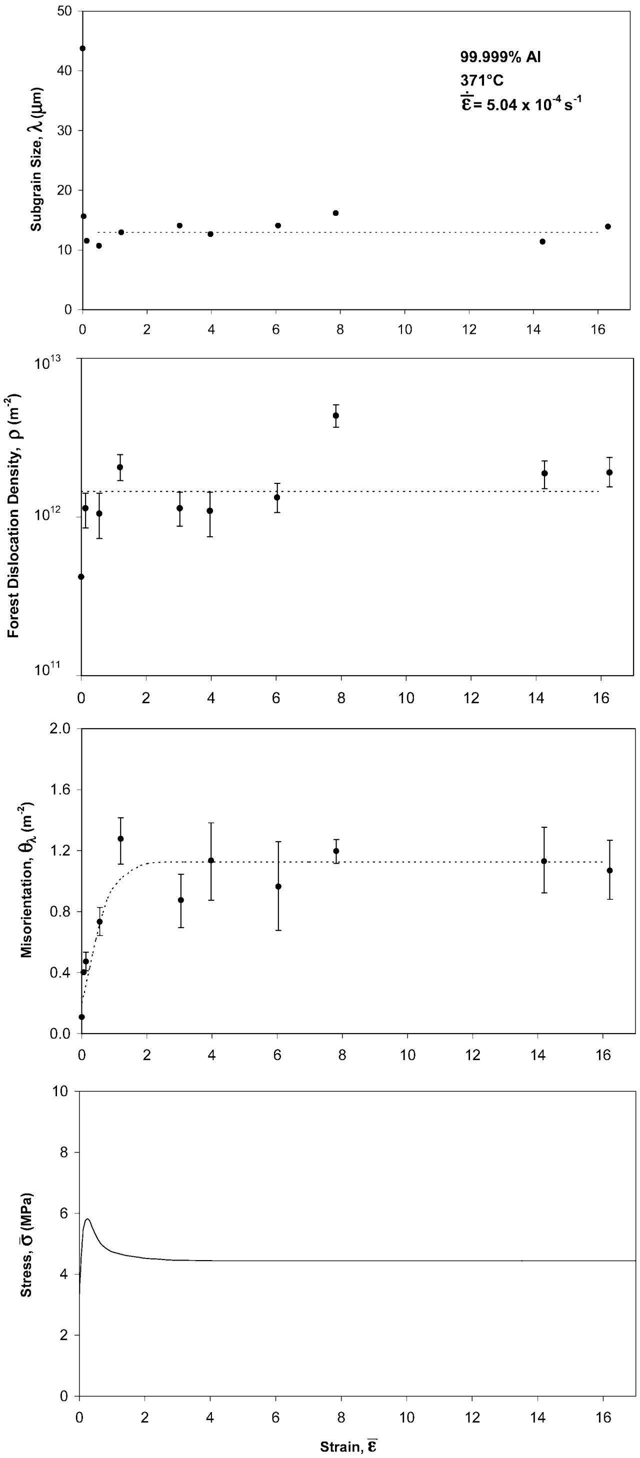


(*a*)

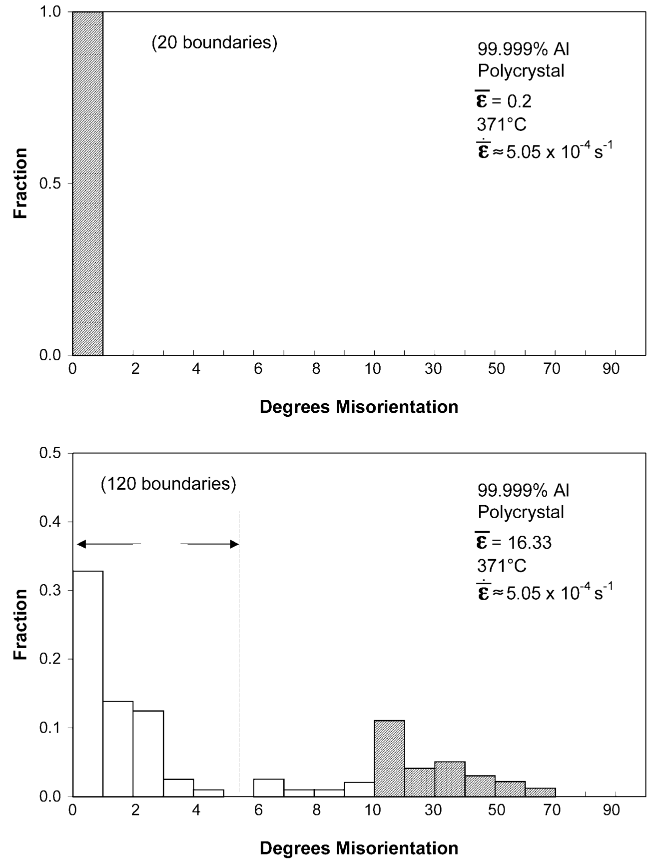


(*b*)

Fig. 2—The dislocation microstructure of pure aluminum deformed to large strains at 371 °C. (*a*) The (equiaxed) subgrain size and density of dislocations not associated with subgrain boundaries are approximately constant once the peak stress (steady state in tension) is attained. The misorientation of subgrain boundaries that are presumed to form only from dislocation reaction ($\theta_\lambda$) increases during early steady state and then remains constant. (*b*) The histogram shows that at the peak stress, nearly all boundaries are of low misorientation. By a strain of 4 (and up to 16), nearly one-third of the subgrain facets are HABs, but these are believed to result from the original HAB of the starting polycrystal through GDX.

torsion axis). However, Taylor factor analysis reveals that if textures are responsible for the softening, then the compressive (again, the compression axis is parallel to the torsion axis) yield stresses will be unchanged or *increase* with torsion prestrains. Some OIM is performed to independently assess the increase in HAB area from dislocation reaction, to assess this possible effect on torsional softening.

**Table I. Textures and Taylor Factors**

| Texture | Shear Plane and Direction | Nontraditional Slip[14] | Traditional Slip[27] |
|---|---|---|---|
| A | $(1\bar{1}\bar{1})\ [1\bar{1}0]$ | — | 1.73 |
| $A^2$ | (111) [112] | — | — |
| C | (001) [110] | M = 2.65 | 2.99 |
| $B^1$ | $(\bar{1}12)$ [110] | M = 2.34 | 2.44 |
| Isotropic | — | M = 2.69 | 2.86 |

## II. EXPERIMENTAL PROCEDURE

The Al used in this investigation was provided as rods of 99.999 pct purity. The torsion specimens were annealed at 400 °C for 1 hour. The typical resulting grain size was 0.89 mm, for hollow torsion experiments and elongated, 0.25 by 0.50 mm, grains (long axis parallel to the rod axis) for the solid specimens. Details of the solid torsion specimen testing procedure are described elsewhere.[16] Equivalent uniaxial stress and strain calculations for the solid torsion specimens utilized[28]

$$\bar{\sigma} = \frac{T}{2\pi R^3}(3 + n + m)\sqrt{3} \qquad [1]$$

where $T$ is the applied torque, $R$ is the specimen radius, $n$ is the strain-hardening exponent ($n = 0$ at steady state), and $m$ is the strain-rate sensitivity exponent (assumed = 0.225 for Al at steady state). The strain at the outer radius is

$$\bar{\varepsilon} = \frac{R\,\theta}{l\sqrt{3}} \qquad [2]$$

where $\theta$ is the angle of twist and $l$ is the gage length. Compression specimens that were extracted from quenched solid specimens (25.4-mm length and 5.1-mm diameter) had a compression axis that was coincident with the original torsion axis and an aspect ratio (length/diameter) = 1.0.

The hollow torsion specimens were tested on an Instron (Canton, MA) 8513 servohydraulic biaxial testing machine. The outer diameter was 8.89 mm and the inner diameter was 4.76 mm. The gage length, $l$, was 2.54 mm. Equivalent-uniaxial (von Mises) stress and strain were calculated from the torque and angle of displacement using[26]

$$\bar{\sigma} = \frac{3T\sqrt{3}}{2\pi(R^3 - r^3)} \qquad [3]$$

$$\bar{\varepsilon}_m = \frac{r_m\,\theta}{l\sqrt{3}} \qquad [4]$$

where $r_m$ is the mean radius and $\bar{\varepsilon}_m$ is the mean strain. An advantage of the hollow specimens is that there is less of a strain gradient than with solid specimens, and this may lead to less ambiguous stress measurements. The specimen dimension, high metal purity, and relatively low strain rate selected negated the effects of adiabatic heating.[29] Some studies may have observed larger (30 pct) softening due to these effects.[9] Compression tests for the quenched specimens (ambient temperature tests) used a 0.2 pct plastic strain offset and a strain rate of $1.67 \times 10^{-4}\ s^{-1}$. The high-temperature compression tests of the hollow specimens used a 0.10 strain offset to mitigate any unanticipated compliance. The elevated-temperature compression tests were performed within 5 seconds of unloading from torsion. The (hollow) compression test strain rate was $5.04 \times 10^{-4}\ s^{-1}$. The compression tests did not account for any constraints (high-temperature tests) nor friction (low-temperature tests).

Orientation imaging microscopy sample preparation consisted of grinding on 4000 grit SiC paper followed by final polishing with colloidal silica and $Al_2O_3$ until a mirrorlike surface was obtained. The remaining surface deformation layer was removed by electropolishing at −25 °C and 37 V using a perchloric (20 pct) and ethanol (80 pct) electrolyte. This study utilized OIM software (INCA/Oxford Instruments) and hardware (Oxford Instruments) that was installed on a PHILIPS* scanning electron microscope (SEM) at the University of California at San Diego. Electron interactions within approximately 50 nm of the sample surface (tilted 70.8 deg) produce Kikuchi patterns on a phosphor screen in the SEM sample chamber. The electron beam scans, point by point, the selected area in the sample, and the orientation data are acquired and stored along with the location of each point on the sample surface. A CCD camera captures these patterns, which are then analyzed and indexed, and, thus, the local lattice orientation relative to the sample axes is unambiguously identified. Orientation maps are constructed, in which each orientation is assigned a color. The OIM map enhancement was performed in order to reduce the effects of pattern overlap in the vicinity of grain boundaries.

*PHILIPS is a trademark of Philips Electronic Instruments Corp., Mahwah, NJ.

Some X-ray diffraction measurements were performed at CSIC-CNIM (Madrid, Spain). X-ray texture measurements were performed on hollow specimens deformed to strains of 0.2, 0.69, and 1.21. Texture measurements were taken in the plane parallel to the shear plane. X-ray texture analysis was performed by the Schulz reflection method using a SIEMENS* D5000 diffractometer furnished with a closed eulerian cradle, using $\beta$-filtered Cu $K_\alpha$. The penetration of this radiation in Al was approximately 70 $\mu$m. The surface area examined was about 1 mm$^2$. The polar angle ranged from 0 to 85 deg in steps of 3 deg. Calculated pole figures were obtained with the SIEMENS DIFFRAC/AT software, using the measured incomplete {200}, {220}, and {111} pole figures. From the pole figures, the even part of the three-dimensional orientation distribution function (ODF), a function of the Euler angles $\phi_1$, $\Phi$, and $\phi_2$, was calculated by a harmonic series expansion method. The odd coefficients were approximated by an iterative procedure. The maximum rank of even and odd coefficients is 22 and 21, respectively. Sample surface preparation consisted of fine grinding using 4000 grit SiC paper and mechanical polishing with diamond powder of grain sizes 6, 3, and 1 $\mu$m. Final polishing was performed using a colloidal silica solution.

*SIEMENS is a trademark of Siemens, AG Munich.

All torsion tests were performed at 371 °C and a strain rate of $5.04 \times 10^{-4}\ s^{-1}$, just as with Figure 2. This ensures that the microstructural development is already well understood, and DRX effects are expected to be nonexistent.

## III. RESULTS

Figure 3(a) illustrates the observed equivalent uniaxial stress, $\bar{\sigma}$, *vs* equivalent uniaxial strain, $\bar{\varepsilon}$, of solid Al deformed in torsion at 371 °C at an equivalent uniaxial strain rate of 5.04 × $10^{-4}$ $s^{-1}$. Three categories of tests are also reported in Fig. 3 and Fig. 4.

(1) T-Q-T tests in which specimens are torsionally deformed at elevated temperature to various strains within the softening regime, quenched to preserve the microstructure, and then torsionally deformed at ambient temperature (coincident with the elevated-temperature straining) to plastic yield.
(2) T-Q-C tests in which specimens undergo elevated-temperature torsion deformation to various strains, followed by a quench, and ambient-temperature compression tests in which the compression axis is coincident with the elevated-temperature torsion axis. The plane of maximum resolved shear stress changes from 90 deg to the torsion axis to 45 deg to the axis. The compression specimens are cut and machined from the quenched torsion specimens.
(3) T-HT-C tests in which *hollowed* torsion specimens undergo elevated temperature deformation followed by *elevated* temperature compression. Tests are similar to (2) but with a smaller strain gradient and compression deformation at the same temperature as torsion tests.

If the softening is due principally to texture or (isotropic) microstructural effects, then the ambient-temperature torsion tests that follow the elevated-temperature tests should show a reduction in yield stress with increasing elevated-temperature prestrain within the softening regime. Figure 3(b) shows the results of eight T-Q-T tests. Some scatter is present of uncertain origin, perhaps nonuniform quenching. With elevated temperature prestrain, the ambient-temperature yield stress decreases by roughly 15 to 20 pct, as expected. If the softening is due to a change in mechanism (*e.g.*, GBS, Coble creep, *etc.*), then the ambient temperature decrease in yield stress with prestrain would not be expected. The T-Q-C tests are reported in Figure 3(c). Fourteen compression specimens were extracted from five torsion specimens tested to various elevated-temperature strains. Interestingly, the data show a trend of *increasing* ambient-temperature compressive yield strength with increasing elevated temperature prestrain within the softening regime. The increase is about 10 pct, although some scatter is present, again, of uncertain origin. If the elevated temperature softening is due to a change in (isotropic) microstructure, then the ambient temperature compression tests should show a decrease rather than an increase in strength with elevated-temperature prestrain. The observed trends are, perhaps, most easily explained by the development of a texture at elevated temperature. This will be discussed more later.

Figure 4 illustrates the 16 pct softening of a hollow torsion specimen to a strain of about 1.3. Some small, additional softening might have occurred with additional strain according to Figure 1. However, the limited angle of twist of the torsion equipment precluded larger strains. The behavior is quite similar to that of the solid specimens. The elevated-temperature torsion tests consisted of deformation to various strains within the softening regime. The tests were terminated at three strain levels, the peak-stress strain of about 0.2, 0.46, and the nearly fully softened state at a strain of about 0.69. Upon termination of the tests, specimens were quickly unloaded and compressed. The elevated-temperature compressive stress increases with torsion prestrain in the

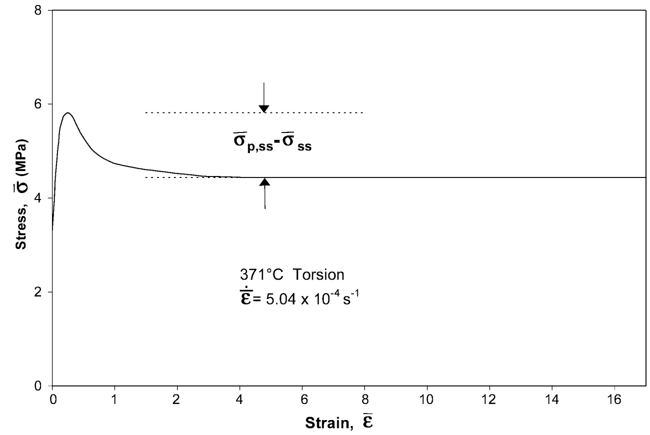


(*a*)

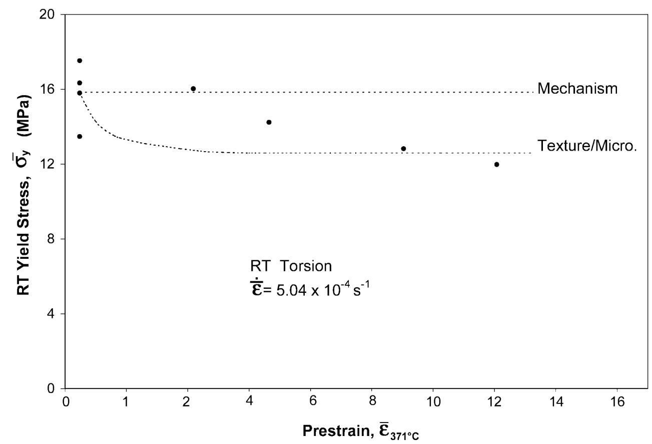


(*b*)

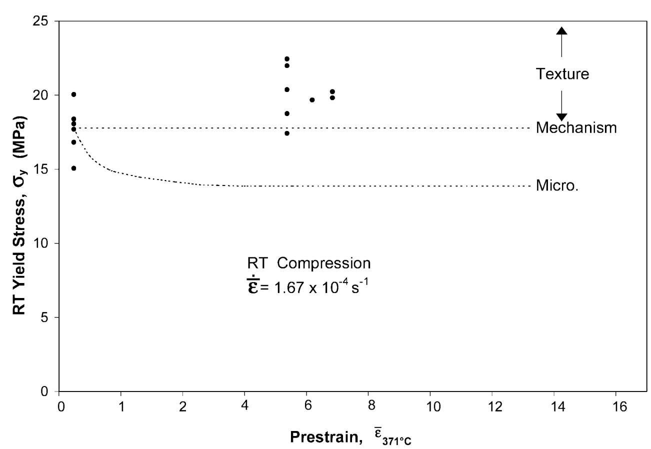


(*c*)

Fig. 3—(*a*) The equivalent uniaxial stress *vs* equivalent uniaxial strain of solid specimens of Al deformed in torsion at 371 °C. (*b*) The ambient temperature torsional yield stress of Al predeformed to various strains in torsion at 371 °C. The ambient temperature yield stress decreases coincidentally with elevated-temperature prestrain, indicating a change in deformation mechanism is not responsible for the elevated-temperature shear softening. (*c*) The ambient temperature compression yield stress of solid Al predeformed to various strains in torsion at 371 °C. The compression axis is coincident to the prior torsion axis. The slight increase in yield stress with elevated temperature suggests that essentially all of the elevated-temperature shear stress reduction is due to a decrease in the Taylor factor.

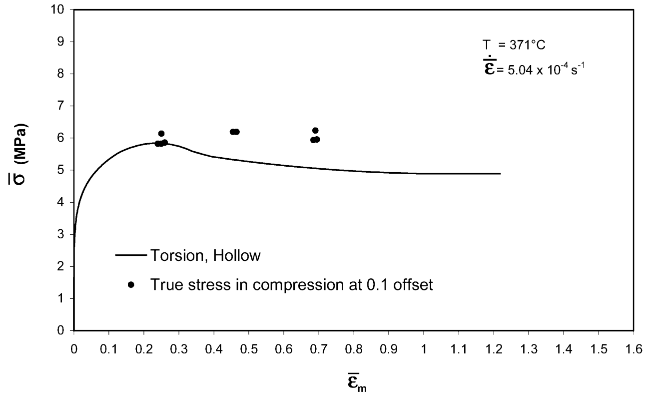


(*a*)

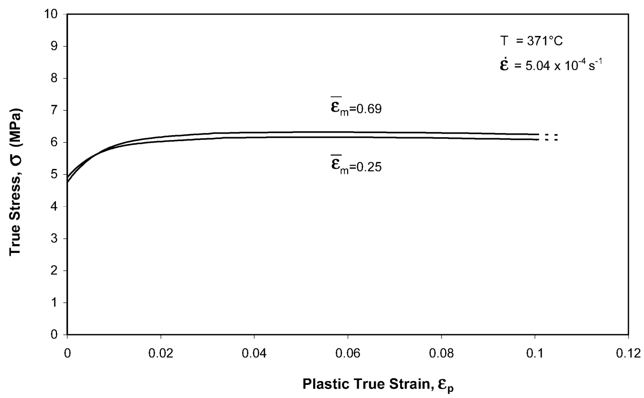


(*b*)

Fig. 4—(*a*) The 371 °C equivalent uniaxial stress *vs* equivalent uniaxial strain of hollow torsion specimens and the corresponding compressive yield stress (0.10 strain offset) at the same strain rate and temperature subsequent to various (pre)strains in torsion. Again, the slight increase in strength suggests that the shear stress decrease is due to decreases in the Taylor factor. (*b*) The stress *vs* strain behavior of two compression tests with different torsion prestrains.

softened regime. The increase is less than that of the unhollowed ambient-temperature compression tests. The explanation for this is not known. [Compression stresses are slightly higher than the peak torsion stresses. This may be partly due to (unaccounted) constraint in compression or other[30] effects.]

If the "fully softened" regime specimens are compressed along the torsion axis, the average Taylor factor for the $A^2$, C, and $B^1$ textures (calculated with the aid of Figure 5 from[31]) would be 3.06 (7 pct increase). If just the $B^1$ texture is used, a Taylor factor of about 3.1 is obtained and an 8 pct increase is expected (C is associated with a fairly low factor of about 2.45). The A texture[5] would be relatively high at 3.67. All four components[6] suggest about a 13 pct increase, nearly identical to the increase observed in 3(c). Thus, based on the observed textures in pure Al, we expect about the same value or up to 28 pct higher of the Taylor factor for the compression tests on the prior-torsionally deformed (textured) specimens as for a random array of polycrystals deformed in compression (microstructural effects omitted). [Pettersen would appear to predict based on equal $B^1$ and C components, a 3 pct drop using traditional slip, although additional microstructural softening (over 10 pct) would also occur.] Therefore, based on this procedure,

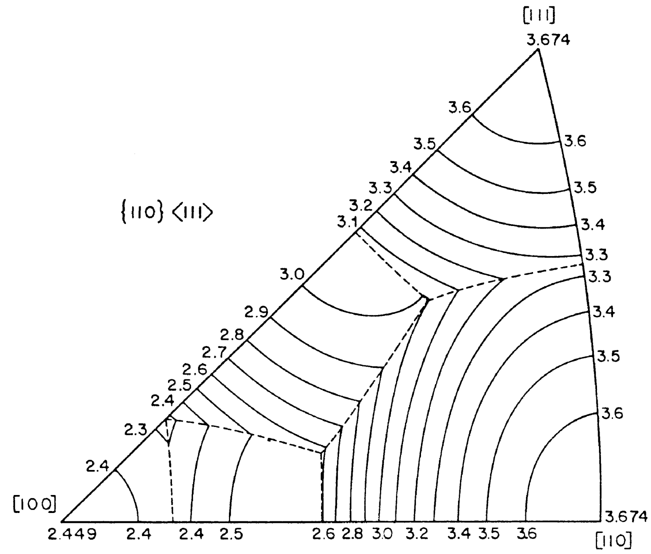


Fig. 5—Contours of the Taylor factor, M, for {111} ⟨110⟩ slip.[32]

the ambient temperature compressive flow stresses of pretorsionally deformed Al are not expected to decrease if ($A^2$, C, $B^1$) or (A, $A^2$, B, C) textures are equally present or if the $B^1$ texture dominates. Therefore, our experimental results appear basically consistent with the predictions of a dominating texture explanation for elevated temperature softening. Also, only hardening is observed at elevated temperature in the Al single-crystal experiments[15,19] in which the torsion axis was coincident with the soft [111], as would be expected according to the texture explanation. With the single crystals, 9 pct of subgrains become HABs with large strain deformation (about 35 pct for polycrystals) and the flow stress does not decrease, as might be suggested by others. Interestingly, Schmidt *et al.*[32] deformed a ferritic stainless steel to very large strains at elevated temperature, observed flow softening, and also observed that the ambient compressive yield stress increased slightly with elevated temperature prestrain, just as with Al in the present investigation. (Some of their softening may be adiabatic heating from a relatively high strain rate, stress, and high specimen aspect ratio. They did not, however, report a texture but did report an increase in HAB area.)

Texture and subgrain and grain-boundary misorientation were assessed using OIM and X-ray diffraction. Because of the large starting grain size, especially in comparison with the torsion specimen wall thickness, only 10 to 20, or so, grain orientations could be determined from each specimen by OIM. Thus, the statistics of textures in this metal may not allow a very meaningful comparison with textures of more fine-grained specimens. The texture by X-ray diffraction was measured at 0.20, 0.69, and 1.2 strain. The {100} and {110} fiber textures were observed with {031} ⟨100⟩ replacing the {110} fiber texture at 1.21 strain. The {100} became stronger as a function of strain. Overall, the OIM results did not conclude strong A, B, or C textures being present, which is a weakness of this investigation. A definitive Taylor factor was not determined, and it was unclear whether a 15 to 20 pct drop would be predicted as with most other torsion studies. Figure 7 illustrates the orientation of several (10 to 20) grains at 0.69 strain. The OIM was also used to assess grain size as a function of strain. Grain

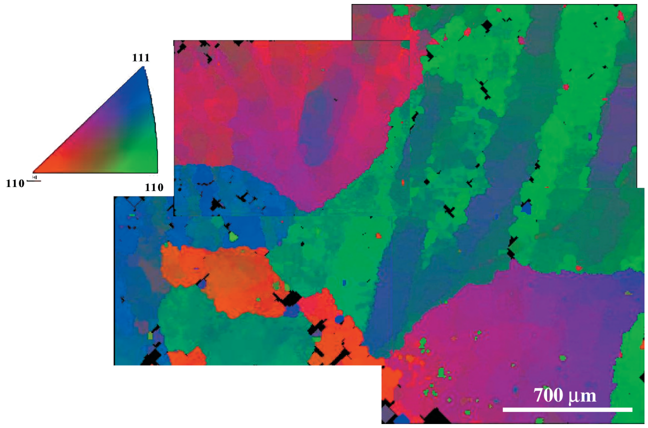


(*a*)

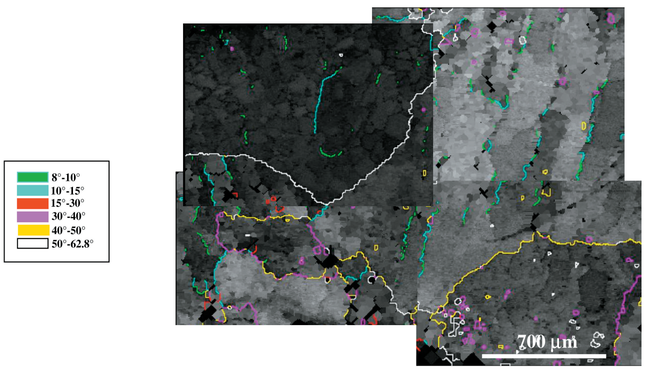


(*b*)

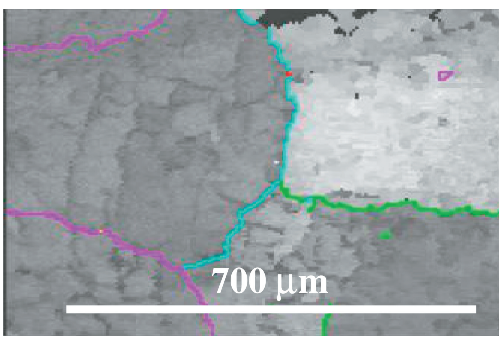


(*c*)

Fig. 6—OIM map of the shear plane of pure Al deformed to (*a,b*) 0.20 and (*c*) 0.69 strains at 371 °C. The original HABs of the polycrystal are visible along with subgrain facets with misorientations greater than 8 deg.

size measurements were performed using the linear intercept method on orientation maps in which only boundaries with misorientations higher than 8 deg were highlighted. As an example, Figure 6 shows the OIM map where the grain size measurements were performed in the samples strained in torsion at 0.2 and 0.69. Grain size measurements mandated OIM as HABs may form with strain as with single crystals.[15] The grain size measurements obtained were 700 $\mu$m (0.2 strain) and 380 $\mu$m (0.69 strain) with a starting (0-strain) grain size of 890 $\mu$m.

Interestingly, some HABs ($\theta > 8$ deg) appear to form from shear, but not as a result of any DRX (or GDX). These may only slightly decrease the (effective) grain size from that of the starting annealed state to 700 $\mu$m at 0.20 strain.

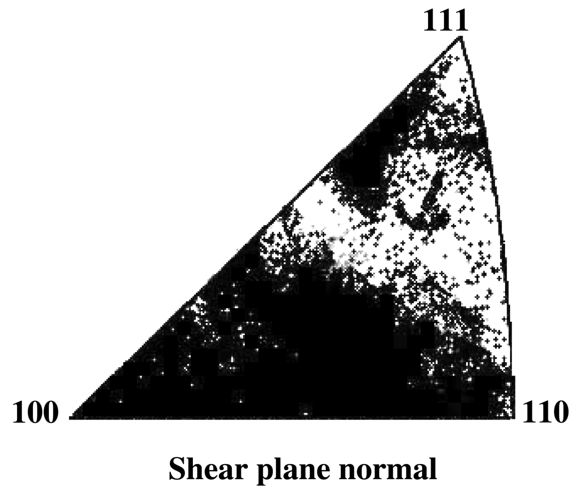


(*a*)

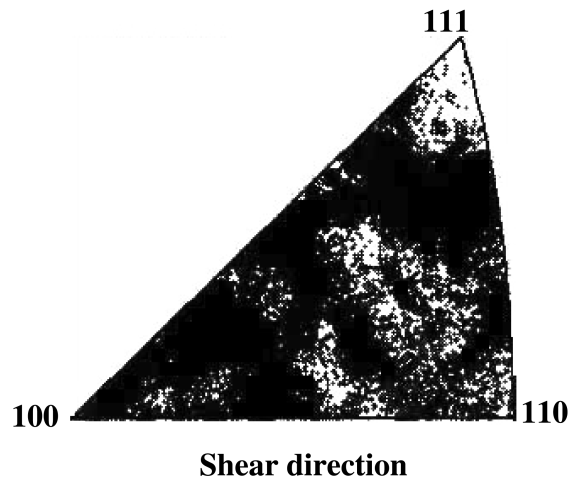


(*b*)

Fig. 7—The (*a*) shear plane normal and (*b*) shear direction, inverse stereographic triangles for hollow torsion specimens deformed to 0.69 strain, as determined by EBSD.

By a strain of 0.69, the size has decreased by roughly a factor of 2 to 380 $\mu$m, but this is expected based on geometric considerations without the formation of new HABs beyond those observed at 0.20 strain. In fact, Figure 6 illustrates no dramatic increase in HABs from 0.2 to 0.69 strain. This decrease in grain size by the established Hall–Petch relationship[31,33] implies a slight *increase* in stress at 371 °C. Furthermore, the aluminum has undergone most of the (17 pct) torsional softening by a strain of 0.69; yet the grain size is *larger* than that of the Al of Figure 2 that *subsequently* experiences 17 pct softening. Hence, the arguments of Pettersen and Nes that most of the torsional softening is due to increased (subgrain size due to) dynamic recovery in response to the increase in high-angle boundary area that is observed with torsional deformation do not appear convincing. Eventually, the specimen of Figure 7, with much larger strain (*e.g.*, 8), will have a very reduced effective grain size (*e.g.*, on the order of 30 to 60 $\mu$m), but *without* any further expected softening. Finally, it should be mentioned that the small isolated "crystallites" that are observed in Figures 6(a) and (b) appear to be artifact from uneven electropolishing.

## IV. DISCUSSION

The fact that a pronounced (macro) texture was not observed (over 0.2 to 0.69 strain) in this study renders the exclusive conclusion of softening by texture, less than very firm. The texture experiments referenced have generally relied on much larger strains than 0.69. It is expected that with larger strains in our (hollow) specimens, the same textures would be observed. These textures give an "average" Taylor factor over the bulk that is consistent with the torsional softening and the compression trends. Softening by DRX has been eliminated, and the remaining possibility for softening is increased recovery due to the increase in HAB area from GDX and any new boundaries formed from dislocation reaction. Figure 6(a) shows some of these new HABs ($\theta = 8$ to 15 deg) formed within the grain interiors (interestingly, rotating sections of the grains to "soft" {111} orientations). However, as mentioned earlier, the total amount of HAB area by a strain of 0.69 seems too small to rationalize softening.

One relevant point for both the "texture" and "recovery" explanations is the heterogeneous nature of plasticity, particularly in coarse-grain Al. For example, Figure 6(a) illustrates large grains in which "bands" of deformation both lead to what appears to be regions of low M and new HABs. Our average Taylor factor analysis was based on the *entire* specimen volume. Thus, it is conceivable that those portions of the specimen accommodating the strain may comprise a smaller volume with a lower Taylor factor that is obscured by the more random texture of the remaining volume. With very large strains and a "homogenization" of the sample deformation, the bulk texture may be reflective of the operating slip systems. If this is the case, then all of the evidence of this study would be fully consistent with the texture explanation. However, proponents of the "recovery" argument (leading to softer microstructures) could invoke analogous reasoning. That is, deformation is initially heterogeneous, and those regions under deformation have relatively high fractions of HABs ($\theta > 8$ deg) in their vicinity (*e.g.*, Figure 6(a) and (b)). Thus, it appears that both the texture and recovery explanations require heterogeneous deformation over the "early" (0.2 to 0.69) strains to rationalize the softening observations of the hollow large-grain torsion specimens. McQueen *et al.*[9,10] show that at 400 °C, commercial purity Al deformed to a strain of 3, 2-mm grain size has much less pronounced (but the same) texture than 0.1 mm Al, despite the same softening trends.

The solid specimen results in which ambient temperature torsion and compression tests are performed appear more consistent with the texture explanation. However, arguments in favor of the recovery explanation can be made to rationalize these observations. If softening were due to decreased dislocation substructure hardening due to increased dynamic recovery through HABs, then the increase in compression strength could be due to a slightly increased contribution of room-temperature strength provided by HABs over that at elevated temperature that also overcompensates the decreased dislocation-structure strengthening. It has been established that the Hall–Petch constant *increases* by a factor of 5 to 10 from 370 °C to ambient temperature[33,34] and dislocation substructure strengthening may not increase by this factor. The (inconsistent) decrease in room temperature torsion tests is, then, more difficult to rationalize by the recovery argument, but perhaps the slip length in torsion is less than that in compression in terms of HABs, so that HAB strengthening is observed at ambient temperature in compression but less substantially in torsion. It is suggested that by GDX, the HABs, by the strain of 4 to 6 in Figure 1, would lie preferentially in the shear plane. Similar arguments have been suggested by others for analogous cases.[31]

The lack of softening with torsional prestrain of the high-temperature compression tests could be rationalized by recovery proponents by suggesting that in compression new slip systems are, of course, activated and these would not have the HABs of the original torsion systems, particularly according to the "heterogeneous" deformation arguments. In summary, however, it appears that, although a dominating influence of HABs on flow softening is possible, the argument appears tenuous.

## V. CONCLUSIONS

Aluminum deformed in torsion at elevated temperature reaches a broad "peak" stress and then undergoes about a 17 pct decrease in flow stress with deformation to roughly 1 to 2 equivalent uniaxial strain. Beyond the strain, the flow stress is approximately constant. The OIM and mechanical tests were performed to better understand the basis of the softening.

1. Experiments were performed where specimens were deformed in torsion to various strains within the softening regime followed by compression tests at ambient and elevated temperature where the compression axis was coincident with the torsion axis. The compressive strength remained constant or even increased with increasing torsional prestrain in the softening regime. Analysis of the compressive yield strengths indicate that the softening is substantially explained by a decrease in the average Taylor factor during elevated temperature torsional deformation.
2. The OIM measurements indicate that some new HAB form from dislocation reaction during deformation within the softening regime, but the small number appear insufficient to rationalize an effect on softening through increased dynamic recovery. Less strong texture development was evidenced in hollow specimens deformed to smaller (0.69) strain by X-ray and OIM but may be explained by the heterogeneous deformation, in coarse-grained (1-mm grain size) Al.

## ACKNOWLEDGMENTS

This work was supported by the United States Department of Energy Basic Energy Sciences under Contract No. DE-FG03-99ER-45768. Discussions with Professor E. Nes, Dr. T. Pettersen, and Professor H.J McQueen were very helpful.

## REFERENCES

1. S.P. Belyayev, V.A. Likhachev, M.M. Myshlyaev, and O.N. Senkov: *Phys. Met. Metall.*, 1981, vol. 52, pp. 143-52.
2. V.A. Likhachev, M.M. Myshlyaev, O. Senkov, and S.P. Belyayev: *Phys. Met. Metall.*, 1981, vol. 52, pp. 156-64.
3. M.M. Myshlyaev, O.N. Senkov, and V.A. Likhachev: in *Strength of*

*Metals and Alloys*, H.J. McQueen, J.-P. Bailon, J.I. Dickson, J.J. Jonas, and M.G. Akben, eds., Pergamon, Oxford, United Kingdom, 1985, pp. 841-46.
4. V.A. Likachev, M.M. Myshlyaev, and O.N. Senkov: *Laws of Superplastic Behavior of Al in Torsion*, Institute of Solid State Physics, Chernogolovka, Russia, 1981 (in Russian).
5. C. Perdrix, M.Y. Perrin, and F. Montheillet: *Mem. Et. Sci. Rev. Metall.*, 1981, vol. 78, pp. 309-20.
6. M.R. Barnett and F. Montheillet: *Acta Mater.*, 2002, vol. 50, pp. 2285-96.
7. S. Gourdet and T. Montheillet: *Mater. Sci. Eng.*, 2000, vol. A283, pp. 274-88.
8. H.J. McQueen, E. Evangelista, and M.E. Kassner: *Z. Metallkd.*, 1991, vol. 82, pp. 336-45.
9. H.J. McQueen, O. Knustad, N. Ryum, and J.K. Solberg: *Scripta Metall.*, 1985, vol. 9, pp. 73-78.
10. H.J. Mc Queen, J. K. Solberg, N. Ryum, and E. Nes: *Phil. Mag.*, 1989, vol. 60A, pp. 473-85.
11. H.J. McQueen and W. Blum: *Mater. Sci. Eng.*, 2000, vol. A290, pp. 95-107.
12. H.J. McQueen: *ICOTOM 12*, J.A. Spunar, ed., NRC Research Pub., Ottawa, 1999, pp. 836-41.
13. T. Pettersen: Ph.D. Thesis, Norwegian University of Science and Technology, Trondheim, Norway, 1999.
14. T. Pettersen and E. Nes: *Mater. Sci. Forum*, 2002, vols. 331–337, pp. 601-06.
15. M.E. Kassner: *Metall. Trans. A*, 1989, vol. 20A, pp. 2182-85.
16. M.E. Kassner and M.E. McMahon: *Metall. Trans. A*, 1987, vol. 18A, pp. 835-46.
17. M.E. Kassner, H.J. McQueen, and M.M. Myshlyaev: *Mater. Sci. Eng.*, 1989, vol. 108A, pp. 45-61.
18. M.E. Kassner, N.Q. Nguyen, G.A. Henshall, and H.J. McQueen: *Mater. Sci. Eng.*, 1991, vol. A132, pp. 97-105.
19. M.E. Kassner: in *Hot Deformation of Aluminum Alloys II*, T.R. Bieler, L.A. Lalli, and S.P. McEwen, eds., TMS, Warrendale, 1998, pp. 3-8.
20. H. Yamagata: *Scripta Metall. Mater.*, 1994, vol. 30, pp. 411-16.
21. R.D. Doherty, D.A. Hughes, F.J. Humphreys, J.J. Jonas, D. Juul Jensen, M.E. Kassner, W.E. King, T.R. McNelley, H.J. McQueen, and A.D. Rollett: *Mater. Sci. Eng.*, 1997, vol. A238, pp. 219-74.
22. D.A. Hughes, M.E. Kassner, M.G. Stout, and J.S. Vetrano: *J. Met.*, 1998, vol. 50, pp. 16-22.
23. M.E. Kassner, H.J. McQueen, and E. Evangelista: *Mater. Sci. Forum,* 1993, vol. 113, pp. 151-56.
24. M.E. Kassner and M.-T. Perez-Prado: *Progr. Mater. Sci.*, 2000, vol. 45, pp. 1-102.
25. G.A. Henshall, M.E. Kassner, and H.J. McQueen: *Metall. Trans. A*, 1992, vol. 23A, pp. 881-89.
26. U.F. Kocks, C.N. Tome, and H.-R. Wenk: *Texture and Anisotropy*, Cambridge Press, United Kingdom, 1998.
27. S.C. Shrivastava, J.J. Jonas, and G.R. Canova: *J. Mech. Phys. Solids*, 1982, vol. 30, pp. 75-90.
28. W.J. McGregor Tegart: *Elements of Mechanical Metallurgy*, Macmillan, New York, NY, 1966.
29. R. Horiuchi, J. Kaneko, A.B. Elsebai, and M.M. Sultan: Report No. 443, Institute of Space and Aerospace Science, University of Tokyo, Tokyo, Feb. 1970.
30. B. Peters, M. Siefeldt, C. Teodosiu, S.R. Kaleninde, P. van Houtte, and E. Aernoudt: *Acta Mater.*, 2001, vol. 49, pp. 1607-19.
31. G.Y. Chin and W.L. Mammel: *Trans. AIME*, 1967, vol. 239, pp. 1400-05.
32. C.G. Schmidt, C.M. Young, B. Walsec, R.H. Klundt, and O.D. Sherby: *Metall. Trans. A*, 1982, vol. 13A, pp. 447-56.
33. M.E. Kassner and X. Li: *Scripta Metall. Mater.*, 1991, vol. 25, pp. 2833-38.
34. J.T. Al-Haidary, N.J. Petch, and E.R. Delos-Rios: *Phil. Mag.*, 1983, vol. 47A, pp. 863-90.